Coumarin-Based Receptor for Recognition of Zn^{2+} Ion: Spectroscopic Evidence and Imaging Application in Living Cells

Dr. Subarna Guha

Faculty of Chemistry, Central Institute of Plastic Engineering and Technology, Haldia, West Bengal, India

Abstract: **- A fluorescent Zn^{2+} sensor 4-Methyl-2, 6-bis (((2H-chromen-2-one) imino) methyl) - phenol (MCP) based on the 6-aminocoumarin platform has been synthesized. This sensor acts as a highly sensitive and selective fluorescent ON-OFF probe and strong binding ability towards Zn^{2+} in DMSO/water 9:1, v/v (100 mM HEPES buffer; pH 7.4) at room temperature. Other common alkali, alkaline earth and transition metal ions have negligible interference. MCP used for bio-medical applications like living cell imaging at physiological pH using a confocal microscope.**

Keywords: **Fluorescent ON-OFF sensor, Zn^{2+}, coumarin, living cells, Theoretical calculations.**

I. INTRODUCTION

As the second most abundant transition-metal ion in the human body, Zn^{2+} is actively involved in various biological processes [1]. Such as gene transcription, regulation of metalloenzymes, and neural signal transmission [2]. Chelatable Zn^{2+} is present at especially high concentrations in brain,[3] pancreas,[4] and spermatozoa[5]. Chelatable Zn^{2+} regulates neuronal transmission in excitatory nerve terminals, suppresses apoptosis,[6] contributes to neuronal injury in certain acute conditions,[7] epilepsy,[8] and transient global ischemia,[9] seizures,[10] and brain injury [11]. In addition to acute toxicity, disruption of Zn^{2+} homeostasis may play a role in the pathology of several neurodegenerative disorders, [12] like the formation of β-amyloid plaques in Alzheimer's disease [13-14] ischemic stroke, and infantile diarrhea [15]. In particular, compared to other tissues, pancreatic islets contain relatively high concentrations of Zn^{2+}, which play a critical role in insulin biosynthesis, storage and secretion [16]. Hence, the development of Zn^{2+}-probes is a promising field. Rapid progress has been made in the development of fluorescent Zn^{2+}-probes in solution, due to their simplicity, high sensitivity and instantaneous response and based on ion-induced fluorescence changes [17]. However, reports of their intracellular Zn^{2+} imaging are rare [18]. It is desired to develop new fluorescent indicators with improved properties, especially with high efficiency in the spectral visible region and study of Zn^{2+}-probes in cell. Most of the currently reported Zn^{2+} fluorescent sensors have the nature of metal chelation enhanced fluorescence (MCHEF), [19-20] which functions via Zn^{2+} binding-induced emission enhancement. Therefore, there is a huge scope and potential for exploring novel fluorophores for Zn^{2+} sensing.

Although there are many highly effective sensors, most of them often require laborious multistep organic synthesis, which slows the discovery process and causes the prohibitively high cost. While our probe is least expensive as it involves a facile one step reaction with commercially available much cheaper chemicals. Herein we report, the synthesis, and characterization of 6-Amino-coumarin and 2, 6 diformyl paracresol hybrid structure (**MCP**)(Scheme-1), is covalently appended to a Zn^{2+} sensitive OFF–ON fluorescent behavior both in solution and cell. The reason for the observed fluorescence enhancement is in the absence of Zn^{2+} ions, the extent of ICT in the ligand **MCP** is efficient and the fluorescence is effectively quenched. The chelation of **MCP** with Zn^{2+}ion induces reduction of the ICT effect in the ligand, thus unquenching the ligand fluorescence. In addition, the enhancement of fluorescence intensity was due to the formation of a **MCP**. Zn^{2+} complex, which resulted in the selective CHEF effect. In the presence of Zn^{2+}, the C=N conjugation with the phenyl ring is inhibited due to the formation of strong chelation with Zn^{2+} giving rise to intense fluorescence. On the other hand, in general, compounds containing acyclic C=N bonds are nonfluorescent, and cyclic C=N bonds significantly fluorescent [21]. 4-Methyl-2, 6-bis (((2H-chromen-2-one) imino) methyl) - phenol (**MCP**) was designed, in which the C=N bond can react with Zn^{2+} to make the acyclic C=N bond become to cyclic C= N bond, resulting in a fluorescent product. If a fluorescent chemosensor with low fluorescence intensity (off-type) shows a marked enhancement in fluorescence intensity in presence of Zn^{2+} (on-type), it is very sensitive for the detection of Zn^{2+} in living cell. The present synthesis of Zn^{2+} sensor is aimed so achieving these objectives.

II. EXPERIMENTAL

2.1. Materials

4-Methyl-2, 6-diformylphenol was synthesized starting from p-cresol by following a published procedure [22]. Coumarin was available from S. D. Fine Chem. Ltd., India. 6-

aminocoumarin was synthesized starting from coumarin by following a published procedure [23]. Solvents were purified by standard procedure. All other chemicals and solvents were of analytical reagent grade and were used without further purification. Milli-Q Millipore 18.2 M Ωcm^{-1} water was used throughout all the experiments. The sources of Na^{+},Ca^{2+},Mn^{2+},Cr^{3+}, Fe^{3+}, Co^{2+}, Ni^{2+}, Cu^{2+}, Zn^{2+}, Cd^{2+}, $Hg^{2+}$and Pb^{2+} ions are either their chloride, nitrate or perchlorate salts.

2.2. Instrumentation

Spectroscopic data were obtained using the following instruments: UV-Vis spectra were recorded on Shimadzu Multi Spec 1501 absorption spectrophotometer; FTIR spectra (KBr disk, 4000-450 cm^{-1}) by Perkin Elmer FT-IR spectrophotometer model RX-1; Mass spectrum was recorded in QTOF Micro YA 263 mass spectrometer in ES positive mode. Fluorescence emission and excitation spectra were recorded at room temperature (298 K) in aqueous solution with a Hitachi F-4500 spectrofluorometer equipped with a temperature controlled cell holder. Micro analytical data (C, H, and N) were collected on Perkin Elmer 2400 CHNS/O elemental analyzer. All pH measurements were performed with systronics digital pH meter (model 335). Thermo gravimetric analysis was performed on a Perkin Elmer TG/DTA lab system l (Technology by SII). The fluorescence imaging system was comprised of an inverted fluorescence microscope (Leica DM 1000 LED), digital compact camera (Leica DFC 420C), and an image processor (Leica Application Suite v3.3.0). The microscope was equipped with a mercury 50 watt lamp. The ligand and its Zn^{2+}complex have been studied theoretically by Ab initio (Hartee Fock) method to have some insight about the **MCP**- Zn^{2+}interaction by using Gaussian '03 software package [24].

2.3. Synthesis of 4-Methyl-2, 6-bis (((2H-chromen-2-one) imino) methyl) - phenol (MCP)

The compound was prepared by a slight modification of the procedure described previously [25] 4-Methyl-2, 6-diformylphenol was synthesized starting from p-cresol by following a published procedure [26]. 6-Aminocoumarine (0.5g, 6.2 mmol) and 2, 6 diformyl paracresol (0.254g, 3.1 mmol) was taken in dry methanol (15 cm3) and it was refluxed for 8 hours. The reaction mixture was refluxed for 1 h. The solution was filtered, concentrated on a rotaevaporator to dryness. The resulting Schiff base, 4-Methyl-2, 6-bis (((2H-chromen-2-one) imino) methyl) - phenol (**MCP**) is reddish solid. Yield 84%; m.p.133±2°C; ^{1}HNMR (300MHz, $CDCl_3$) (supplementary, Fig.S-1), δ: 1.66(s, 3H), 3.72(s, 1H), 6.36(d, 2H), 6.89(d, 2H), 7.13(d, 2H), 7.26(s, 2H), 7.39(d, 2H), 7.5(d, 2H), 8.42(s, 2H). QTOF –MS ES+, (supplementary, Fig.S-2) displays two signals of m/z 451and 473, which can be assigned as the signals for $[M+H]^{+}$ and $[M+Na]^{+}$, respectively. FT-IR (supplementary, Fig.S-3) (KBr, ν cm-1) ν(CO), 1726; ν(C=N), 1623,UV-Visible spectrum (supplementary, Fig.S-4) in DMSO/water 9:1, v/v (100 mM HEPES buffer; pH 7.4) solution at 298K (λ_{max}, nm (ε, 10^3M^{-1} cm^{-1}), 246(0.391), 263(0.706), 340(0.031), 372(0.071), 382(0.061), 405(0.068). Anal. Calculated for $C_{27}H_{18}N_2O_5$: C, 71.99; H, 4.03; N, 6.22, Found: C, 71.82.; H, 3.99; N, 6.21.

2.4. Synthesis of MCP- Zn^{2+} complexes

Zn $(NO_3)_2$(0.025 g, 0.084 mmol) and **MCP** (0.0378 g, 0.084 mmol) ware taken in a 100 ml round bottom flask dissolved in 20 ml methanol. The mixture was magnetically stirred in air for 6 hr and then refluxed for 25 min whereby a clear solution was formed. On evaporating the solvent the brown colored complex was obtained. The tetra coordination of Zn^{2+} can be satisfied by one ligand and one nitrate groups. The electrospray ionization QTOF-MS ES+ (supplementary, Fig.S-5) mass spectrum of this complex displays signal of m/z 685.07, which can be assigned as the signals for $[M +Na]^{+}$. FT-IR (supplementary, Fig.S-6) (KBr, ν cm-1) ν(C=O), 1724; ν(C=N), 1632, and ν (NO_3^{-}) 1377. UV-Visible spectrum (supplementary, Fig.S-4) in DMSO/water 9:1, v/v (100 mM HEPES buffer; pH 7.4) solution at 298K (λ_{max}, nm (ε, 10^3M^{-1} cm^{-1}), 246(0.391), 263(0.706), 340(0.031), 372(0.071), 382(0.061), 405(0.068). Anal. Calculated for $C_{28}H_{26}N_3NaO_{12}Zn$: C, 49.1; H, 3.83; N, 6.14, Found: C, 49.04; H, 3.79; N, 6.13.

2.5. Measurement procedures

Solutions of Zn^{2+} and **MCP** are mixed in different ratios for subsequent fluorescence measurements. The fluorescence emission intensities are measured at 480 nm while the excitation wavelength is fixed at 430 nm. 1.0 cm quartz cell is used for all the measurements.

III. RESULTS AND DISCUSSION

3.1. Spectral characteristics

The metal-binding behavior of **MCP** has been determined by UV-vis and fluorescence spectroscopic studies. Although **MCP** is not highly water soluble, it can be dissolved in DMSO/water 9:1, v/v was added and all the following studies were carried out in DMSO/water 9:1, v/v (100 mM HEPES buffer; pH 7.4. This protocol is commonly used in many reported Zn^{2+} sensors for intracellular Zn^{2+} imaging [27]. The mode of coordination of **MCP** with Zn^{2+} was investigated by spectrophotometric titration at 25 °C in 100 mM HEPES buffer (pH 7.4). (Supplementary, Fig.S-4) illustrates a typical UV-vis titration curve of **MCP** with added Zn^{2+}. As can be seen from (Supplementary, Fig.S-4), the absorption intensity of **MCP** at 230 nm gradually increases as the concentration of Zn^{2+} increases stepwise. Moreover, a new absorption peak appears at 414 nm in the UV-vis spectrum of the **MCP**-Zn^{2+} system, and its intensity also gradually increases with the addition of Zn^{2+}. The presence of a clear isobestic point implies the conversion of free **MCP** sensor to the only Zn^{2+} complex. This absorption peak is likely to be due to the coordination of **MCP** with Zn^{2+}.

The fluorometric titration of ligand **MCP** (10μM) in DMSO/water 9:1, v/v (100 mM HEPES buffer; pH 7.4 solution exhibits addition of 0.5-20 (μM) concentration of Zn^{2+}ion (Fig.1). Fig.2 represents the emission spectra changes of L (10 μM) upon addition of Zn^{2+} ion. Inset shows the fluorescence image of a solution of the sensors (10 μM) with or without Zn^{2+} (10 μM) ion excited by a commercially available UV lamp. The stoichiometry of the (**MCP**: Zn^{2+} = 1: 1) (Fig.3) of the complex formed between **MCP** and Zn^{2+} ion (host and guest) as evaluated by the method of continuous variation (Job's plot), has also been confirmed by mass spectroscopic determination. The fluorescence quantum yield of **MCP** and [**MCP**-Zn^{2+}] complex were found to be 0.12 and 0.526 respectively [see ESI for details].

3.2. Estimation of binding constant

The unique enhancement of fluorescence is attributed to the strong binding of Zn^{2+}, which is evident from a large binding constant value ($2.75x10^4$) estimated by modified Benesi-Hildebrand equation [28] (Fig.4).

$(1/\Delta F) = 1/\Delta F_{max} + (1/K[C]^n)\ (1/\Delta F_{max})$.

Where $\Delta F = (F_x - F_0)$ and $\Delta F_{max} = F_\infty - F_0$, where F_0, F_x, and F_∞ are the emission intensities of **MCP** in the absence of Zn^{2+}, at an intermediate Zn^{2+} concentration, and at the concentration of complete interaction, respectively. K is the binding constant and C is the Zn^{2+} concentration and n is the number of Zn^{2+} ion bound per **MCP** (here, n = 1).

Fig.5 showed the plot of variation of emission intensities of **MCP** as a function of added [Zn^{2+}], which could also be used for determination of unknown [Zn^{2+}] and also detect as low as 1 μM Zn^{2+} in DMSO/water 9:1, v/v (100 mM HEPES buffer; pH 7.4)solution excited at 430 nm.

Fig.6 shows the effect of pH on the fluorescence intensity of **MCP** (10 μM) maximum at pH 7.4, in the presence of 1.0 equiv. of Zn^{2+} in DMSO/water 9:1, v/v (100 mM HEPES buffer; pH 7.4)at room temperature which makes it suitable for biological application in physiological conditions. Fig. 7 showed that the emission intensity of **MCP**- Zn^{2+}system in DMSO/water 9:1, v/v (100 mM HEPES buffer; pH 7.4) solution remained almost unaltered over a period of 10 minutes.

3.3. Selectivity

The influence of a number of common transition metal ions on the fluorescence intensity of the proposed [Zn^{2+}] selective chemosensor was investigated (Fig.8).The fluorescence intensity of the complex in the presence of Zn^{2+} remained either unchanged or weakened (Fig.9) in the presence of alkali, alkaline earth metals(Na^+,Ca^{2+}) and small changes with transition metal ions (Cd^{2+}, Al^{3+}, Mn^{2+}, Cr^{3+} Co^{2+}, Pb^{2+}, ,Ni^{2+}, Fe^{3+},Cu^{2+}) which indicate that all these metal ions were not coordinating with the donor site of the title compound **MCP**.

3.4. Thermal studies

Stability of the ligand, **MCP** and its Zn^{2+} complex was studied by thermogravimetry (TGA/DTG) to prove the binding event of the ligand, **MCP** with Zn^{2+} ion supplementary materials (Figs.S-7 and S-8).The TGA curves of the Schiff base complexes were carried out within a temperature range from room temperature up to 700°C. The thermal decomposition of Zn^{2+} complexes takes place in several steps as indicated by DTG peaks around 130-170 ºC, and 290-330ºC corresponding to the mass loss of two coordinated water molecules, and nitrate ion , respectively.

3.5. Molecular level interaction

The geometry optimizations were carried out using the Ab initio (Hartee Fock) method with a 6-311G** basis set for the **MCP** and LANL2DZ effective core potential (ECP) basis set for the Zn^{2+} complex is shown in Fig. 10 and Fig. 11 respectively. Distinct differential nature of HOMOs and LUMOs of the **MCP** and these molecular complexes indicates a molecular level interaction between the ligand L and these metal ions. Fig. 12 **MCP** showed the energy gap between highest occupied molecular orbital (HOMO) and lowest unoccupied molecular orbital (LUMO) of the **MCP** and its complex.

Different parameters like, bond moments, dipole moments, quadruple moments along with optimized energies of the **MCP** and its complex were presented in the supplementary data (S-9 to S-12).

3.6. Preparation and imaging of cells

Candida albicans cells (IMTECH No. 3018) from exponentially growing culture in yeast extract glucose broth medium (pH 6.0, incubation temperature, and 37^0C) were centrifuged at 3000 rpm for 10 minutes washed twice with 0.1 M HEPES buffer (pH 7.4). Then cells were treated with Zinc nitrate (1 mg /ml) solution (10 μM) for 30 minutes. After incubation, the cells were again washed with HEPES buffer and then incubated with **MCP** (10 μM) for another 15 minutes. Cells thus obtained were mounted on grease free glass slide and then washed in normal saline and photographed under 100X objective using UV filter in a Leica Fluorescence Microscope after adding **MCP** (Fig.13b). Similarly, freshly collected pollen grains of *Allamanda puberula* (Aapocynaceae, Fig.13d) have been collected, while their respective controls are presented in Fig.13a and Fig.13c respectively. Cells incubated with **MCP** but without Zn^{2+} were used as control. Both Zn^{2+} treated and untreated cells were stained with **MCP** and observed under fluorescence microscope.

Photographs indicate that the **MCP** is easily permeable to the types of living cells tested and harmless (as the cells remain alive even after 30 minutes exposure to the **MCP** at 10 μM concentration). Intensity of the fluorescence is proportional to the concentration of Zn^{2+} present in the cell. Thus **MCP** may be used to detect intracellular Zn^{2+} in living cells.

IV. CONCLUSIONS

We have demonstrated the synthesis of Schiff base compound an efficient and selective fluorescent sensor for trace level detection and estimation of Zn^{2+} ion from aqueous solution. The binding of $Zn^{2+}$is highly selective, allowing for selective detection in the presence of competitive nontransition and transition-metal ions alike. Preliminary computational studies by ab-initio (Hartree Fock) method provided a molecular level interaction between the reagent (**MCP**) and Zn^{2+} ion. Finally, the probe has bio-medical applications like living cell imaging at physiological pH using a confocal microscope.

ACKNOWLEDGEMENTS

Financial support from Central Institute of Plastic Engineering and Technology, Haldia is gratefully acknowledged.

SUPPLEMENTARY DATA

Supplementary data absorption, IR, TOF MS, spectra and Theoretical data of physical parameter obtain from Gaussian 03 of **MCP** & associated complexes are associated with this article.

REFERENCES

[1]. J. M. Berg and Y. Shi, Science 271(1996)1081.
[2]. M. Ebadi, F. Perini, K. Mountjoy and J. S. Garvey, J. Neurochem., 66 (1996) 2121.
[3]. C. J. Frederickson, Int. ReV. Neurobiol., 31(1989)145.
[4]. P. D. Zalewski, S. H. Millard, I. J. Forbes, O. Kapaniris, A. Slavotinek, W. H. Betts, A.D. Ward, S. F.Lincoln and I. Mahadevan, J. Histochem. Cytochem., 42(1994)877.
[5]. P.D. Zalewski, X. Jian, L.L.L. Soon, W.G. Breed, R.F. Seamark, S.F. Lincoln, A.D. Ward and F.Z. Sun, Fertil. Dev., 8(1996)1097.
[6]. A.Q. Truong-Tran, L.H. Ho, F. Chai and P.D. Zalewski, J. Nutr., 130(2000) 1459S.
[7]. D.W. Choi and J.Y. Koh, Annu. ReV. Neurosci., 21(1998)347.
[8]. C.J. Frederickson, M.D. Hernandez and J.F. McGinty, Brain Res., 480(1989)317.
[9]. J.Y. Koh, S.W. Suh, B.J. Gwag, Y.Y. He,C.Y. Hsu and D.W.T. Choi, Science 272 (1996) 1013.
[10]. C.T. Sheline, M.M Behrens and D.W. Choi, J. Neurosci., 20(2000)3139.
[11]. E.C.Yeiser, A.A. Lerant, R.M. Casto and C.W. Levenson, Neurosci. Lett., 277(1999)75.
[12]. S.W. Suh, K.B. Jensen, M.S. Jensen, D.S. Silva, P.J. Kesslak, G. Danscher and C.J. Frederiksson, Brain Res., 852(2000)274.
[13]. C.C. Curtain, F. Ali, I. Volitakis, R.A. Cherny, R.S. Norton, K. Beyreuther, C.J. Barrow, C.L. Masters, A.I. Bush and K.J. Barnham, J. Biol. Chem., 276 (2001) 20466.
[14]. K. Suzuki, T. Miura and H. Takeuchi, Biochem. Biophys. Res. Commun., 285(2001) 991.
[15]. A.I. Bush, W.H. Pettingell, G. Multhaup, M. Paradis, J.-P. Vonsattel, J. F. Gusella, K. Beyreuther, C.L. Masters and R.E. Tanzi, Science 265 (1994)1464.
[16]. A.B. Chausmer, J. Am. Coll. Nutr., 17(1998)109.
[17]. S. Maruyama, K. Kikuchi, T. Hirano, Y. Urano and T. Nagano, J. Am. Chem.Soc.,124 (2002)10650.
[18]. M.Taki, J.L. Wolford and T.V. O'Halloran, J. Am. Chem. Soc., 126 (2004) 712.
[19]. K. Komatsu, K. Kikuchi, H. Kojima, Y. Urano and T. Nagano, J. Am. Chem. Soc., 127 (2005)10197.
[20]. A.P. de Silva, H.Q.N. Gunaratne, T. Gunnlaugsson, A.J.M. Huxley, C.P. McCoy, J.T. Rademacher and T.E. Rice, Chem. Rev., 97 (1997) 1515.
[21]. W.-M. Liu, L.-W. Xu, R.-L. Sheng, P.-F. Wang, H.-P. Li and S.-K. Wu, Org. Lett., 9 (2007) 3829.
[22]. R.R. Gagne, C.L. Spiro, T.J. Smith, C.A. Hamann, W.R. Thies and A.K. Schiemke, J. Am. Chem. Soc.,103 (1981) 4073.
[23]. S. Roy, T. K. Mondal, P. Mitra, E.L. Torres and C. Sinha Polyhedron 30, (2011) 913.
[24]. Gaussian 03, Rev.C.02 (Gaussian Inc., Wallingford CT), 2004
[25]. J.J. Grzybowski and F.L. Urbach, Inorg. Chem., 19 (1980) 2604.
[26]. R.R. Gagne, C.L. Spiro, T.J. Smith, C.A. Hamann, W.R. Thies and A.K. Schiemke, J. Am. Chem. Soc., 103(1981) 4073.
[27]. C. J. Fahrni and T. V. O'Halloran, J. Am. Chem. Soc., 121(1999) 11448.
[28]. H. A.Benesi and J. H. Hildebrand, J. Am. Chem. Soc.,71(1949) 2703.

Legends to figures and tables:

Scheme 1: Synthesis of Zn^{2+} ion selective fluorescent sensor (**MCP**). Reagents and conditions : (i) Dry methanol, reflux, 6 h, 84%.

Figure 1. The fluorometric titration of ligand **MCP** (10μM) with addition of 0.5, 1, 2, 3, 4, 5, 6, 7, 8, 9, 10, 20 (μM) concentrations of Zn^{2+}ion obtained from the emission spectra. Excitation at 430 nm with the pass slit width was 5.0 nm.

Figure 2. Fluorescence changes of **MCP** (10 μM) upon addition of Zn^{2+} ion in DMSO/water 9:1, v/v (100 mM HEPES buffer; pH 7.4) solution. Inset shows the fluorescence image of a solution of the sensors (10 μM) with or without Zn^{2+} (10 μM) ion excited by a commercially available UV lamp.

Figure 3. Job Plot for the determination of stoichiometry of [**MCP** - Zn^{2+}] in solution.

Figure 4. Determination of binding constant of **MCP** (10 μM) with Zn^{2+} (10 μM) by Benesi-Hildebrand (fluorescence method).

Figure 5. Linear relationship between **MCP** (10 μM) in DMSO/water 9:1, v/v (100 mM HEPES buffer; pH 7.4) solution as a function of the concentration of Zn^{2+} with excitation at 430 nm.

Figure 6. Effect of pH on the fluorescence intensity of **MCP** (10 μM) at 520 nm in the presence of 1.0 equiv. of Zn^{2+} in DMSO/water 9:1, v/v (100 mM HEPES buffer; pH 7.4 solution. Excitation was provided at 430 nm. (Ex/Em slit=5.0/5.0 nm)

Figure 7. Stability of the **MCP** - Zn^{2+} system with time.

Figure 8. Emission intensities of **MCP** (10 μM) in presence of different metal ions (10 μM).

Figure 9. Interference of different metal ions on the determination of [Zn^{2+}] with **MCP**. [**MCP**] = [Cr^{3+}] = [foreign alkali, alkaline earth and transition metal ions] = 10 μM.

Figure.10 Stereoscopic view of the ligand (**MCP**)(*ab-initio* studies, Hartee Fock method).

Figure.11 Stereoscopic view of the **MCP**-Zn^{2+} molecular complex.(*ab-initio* studies, Hartee Fock method).

Figure.12 The difference between highest occupied molecular orbital's (HOMO) and lowest unoccupied molecular orbital's (LUMO) of the **MCP**, and **MCP**-Zn^{2+} molecular system.

Figure.13. Fluorescence microscope images of *Candida albicans* cells (IMTECH No. 3018); pollen grains of *Allamanda puberula* (Aapocynaceae) without treated with Zn^{2+} and **MCP**-stained with (10 μM) Zn^{2+} for 30 min under 100X objective lens. Incubation was performed at 40°C.

Electronic supplementary materials (ESI)

Fig. S-1. ^{1}HNMR spectra of **MCP**

Fig. S-2. TOF MS ES (+) of **MCP**

Fig. S-3. TOF MS ES (+) of **MCP**-Zn^{2+}complex

Fig. S-4. FTIR spectra of **MCP**

Fig. S-5. FTIR spectra of **MCP**- Zn^{2+} complex

Fig. S-6. UV –Vis spectra of the ligand **MCP** and **MCP** -Zn^{2+}complex in DMSO/water 9:1, v/v (100 mM HEPES buffer solutions ([**MCP**] = [Complex] = 10 μM.

Fig. S-7. Thermogravimetric analysis (TGA / DTG) of **MCP.**

Fig. S-8. Thermogravimetric analysis (TGA / DTG) of **MCP** - Zn^{2+}complex.

S-9. Physical parameters of the **MCP** generated by Ab initio (Hartee Fock) method.

Table S-10. Various bond lengths, angles and dihedral angles of **MCP** generated by Ab initio (Hartee Fock) method.

S-11. Physical parameters of the **MCP**+Zn^{2+} generated by Ab initio (Hartee Fock) method.

Table S-12. Various bond lengths, angles and dihedral angles of **MCP**+Zn^{2+} generated by Ab initio (Hartee Fock) method.

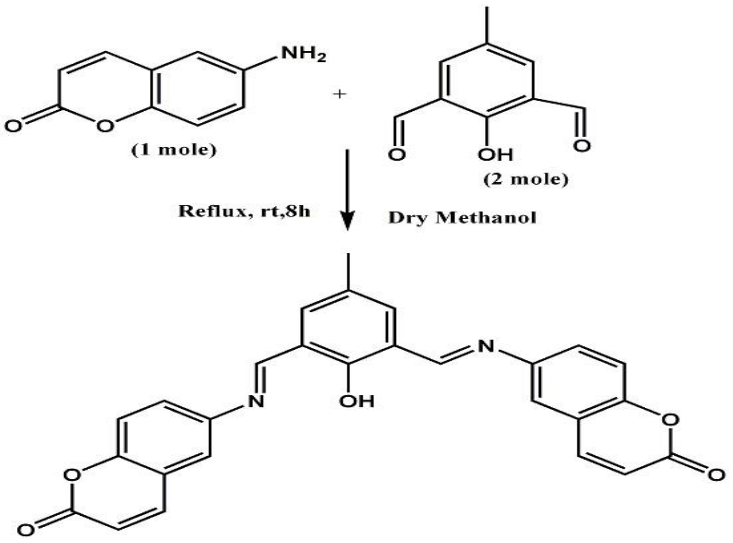

Scheme1

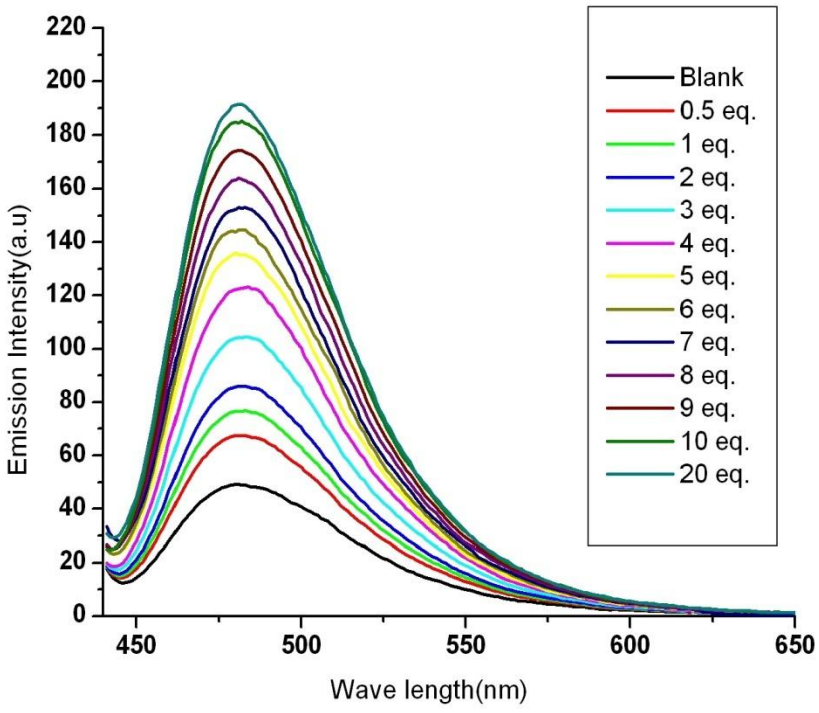

Fig. 1

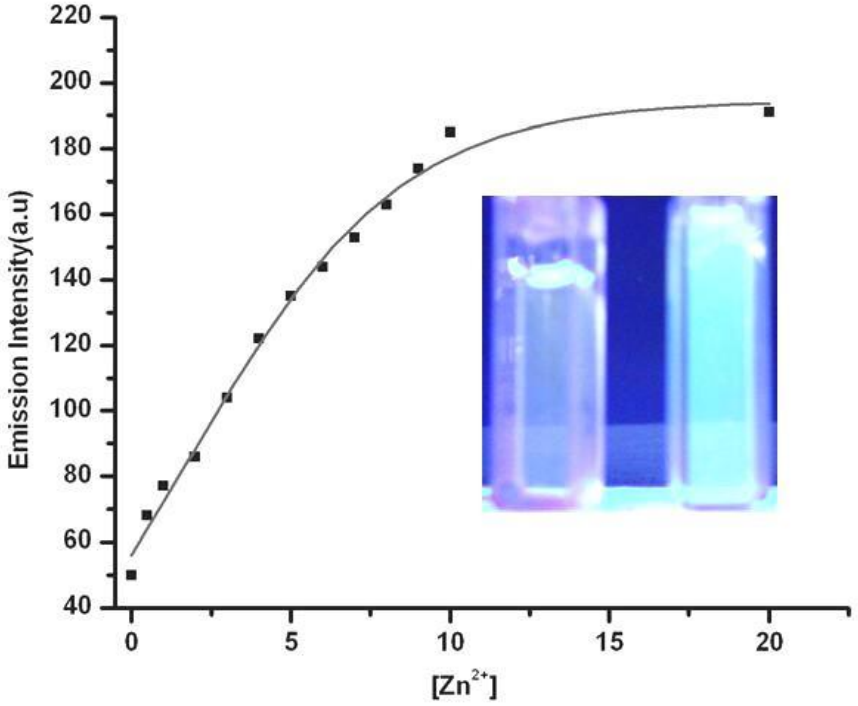
Emission Intensity(a.u)
220
200
180
160
140
120
100
80
60
40
0
5
10
15
20
[Zn2+]

Fig.2

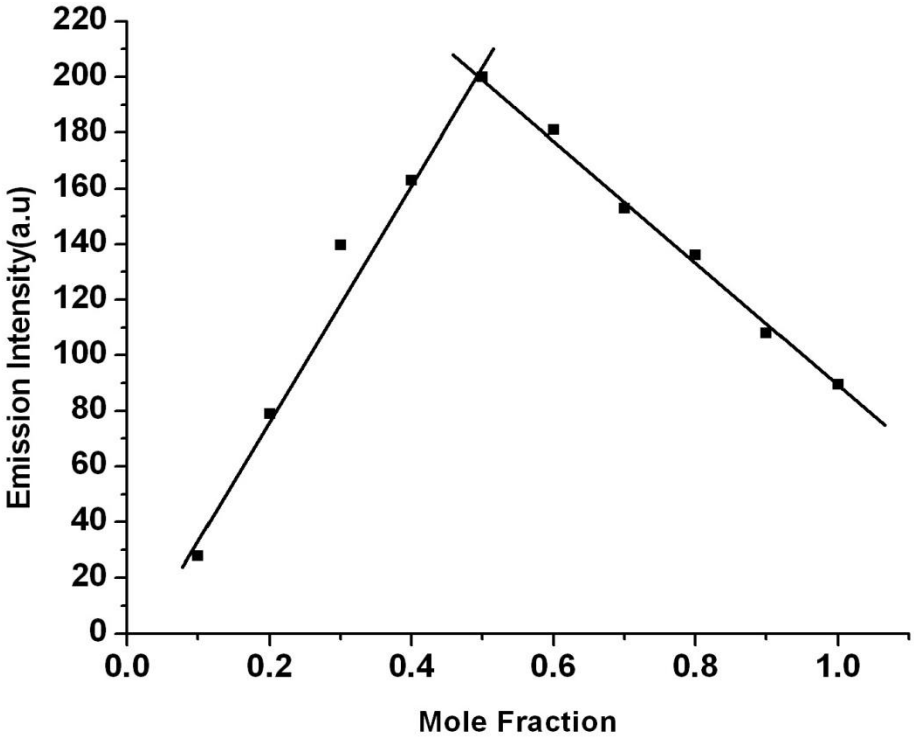
Emission Intensity(a.u)
220
200
180
160
140
120
100
80
60
40
20
0
0.0
0.2
0.4
0.6
0.8
1.0
Mole Fraction

Fig.3

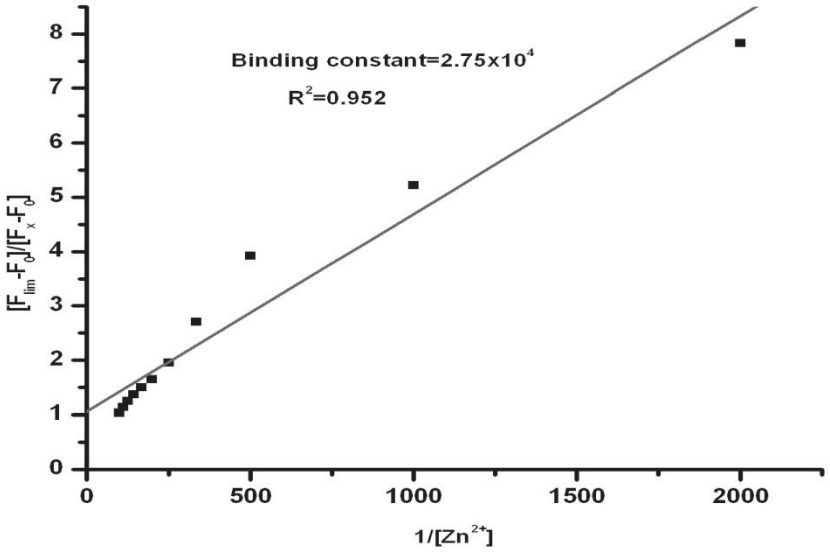

Fig.4

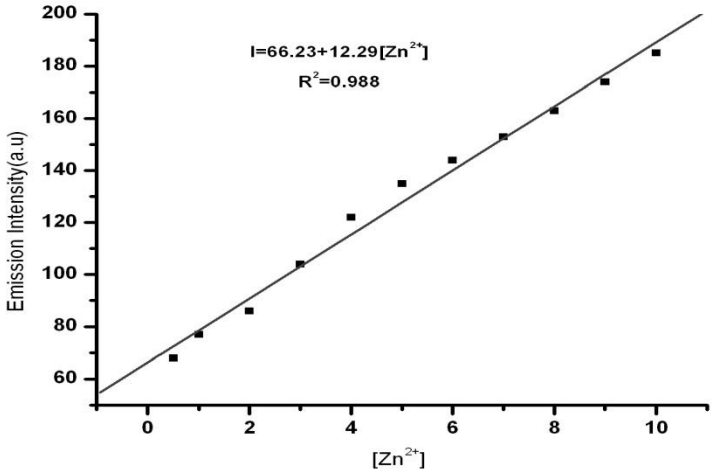

Fig 5

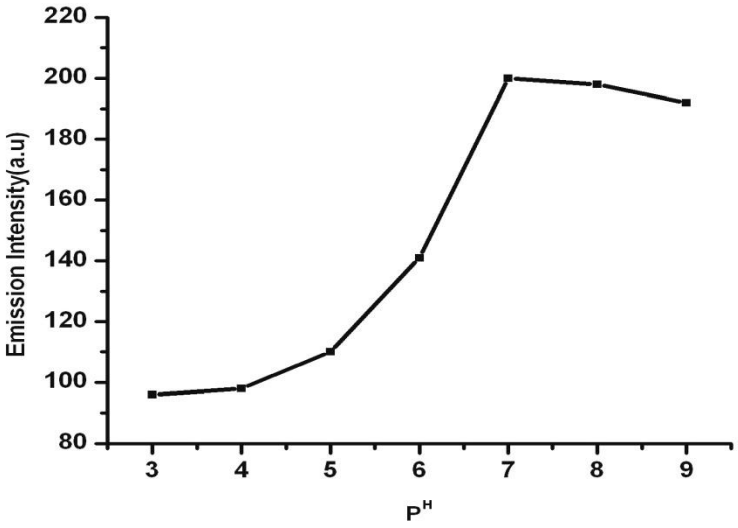

Fig.6

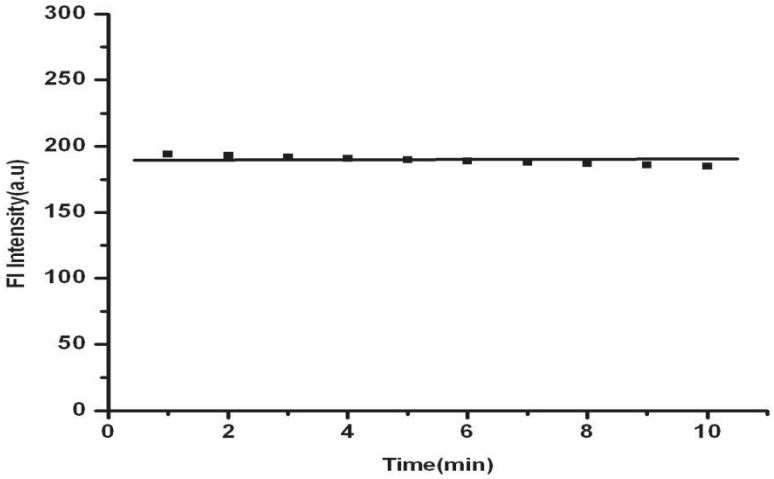

Fig.7

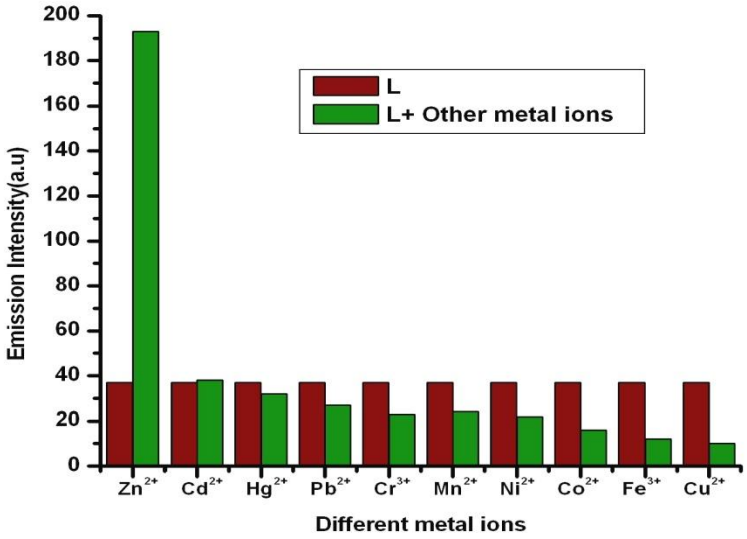

Fig.8

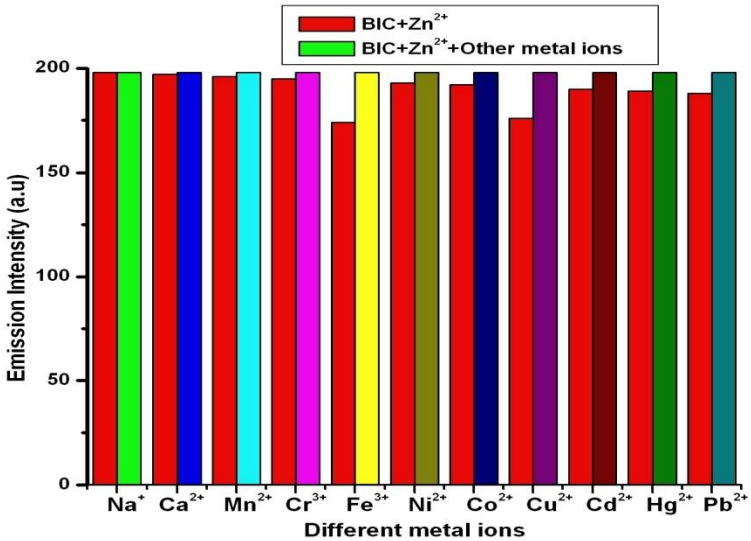

Fig. 9

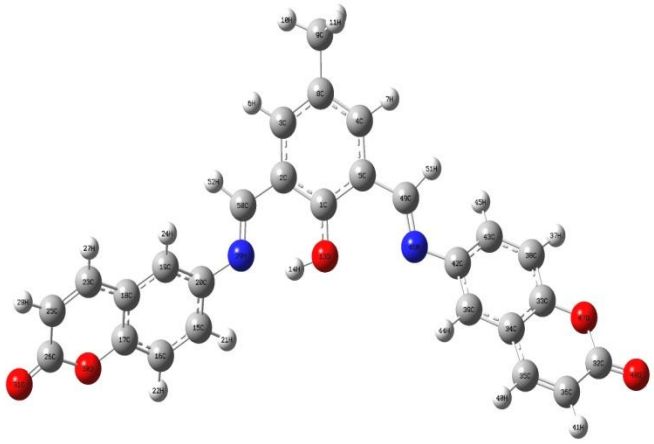

Fig.10

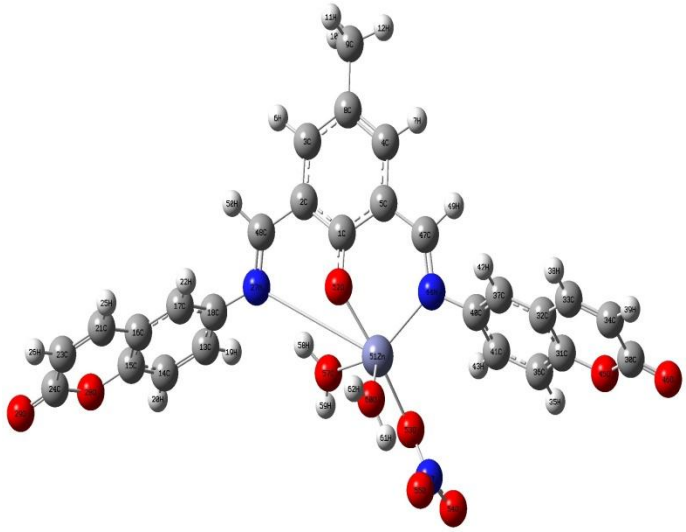

Fig. 11

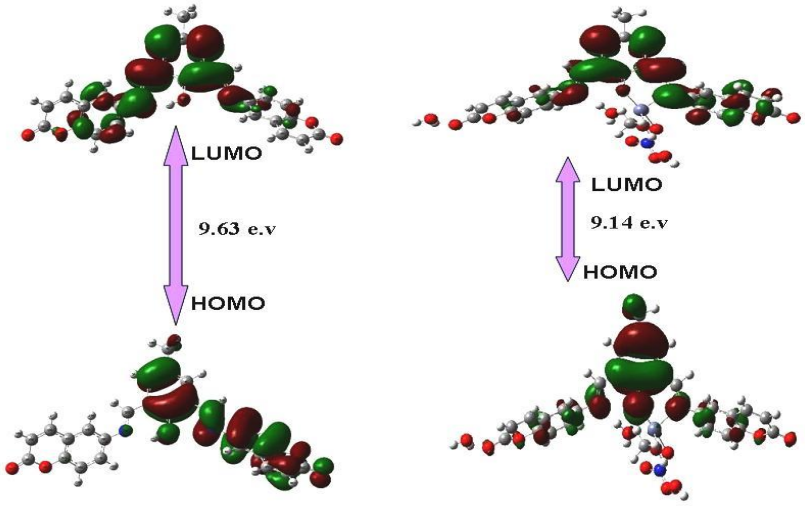

Fig.12

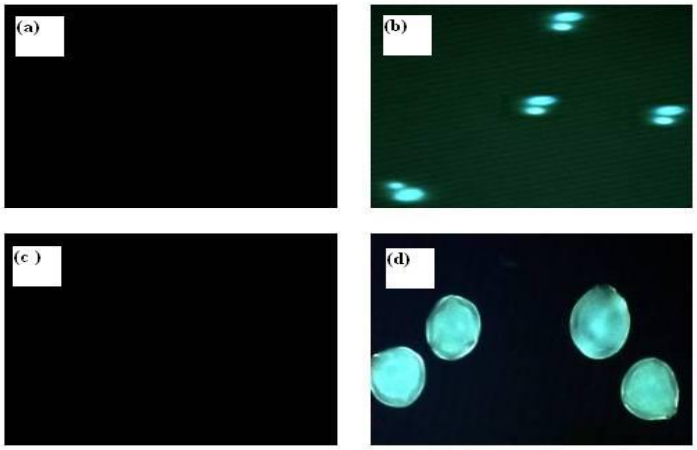

Fig.13

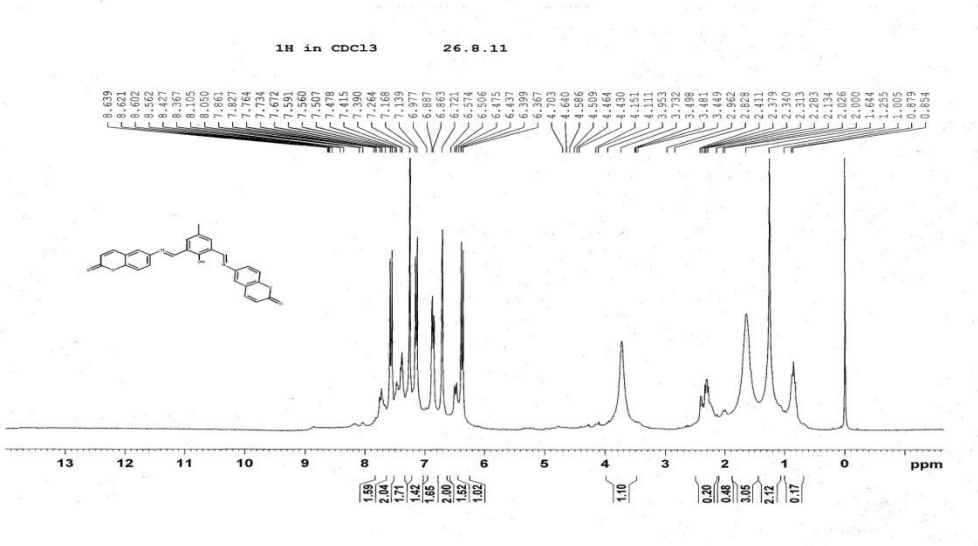

S-1. [1]HNMR spectra of MCP

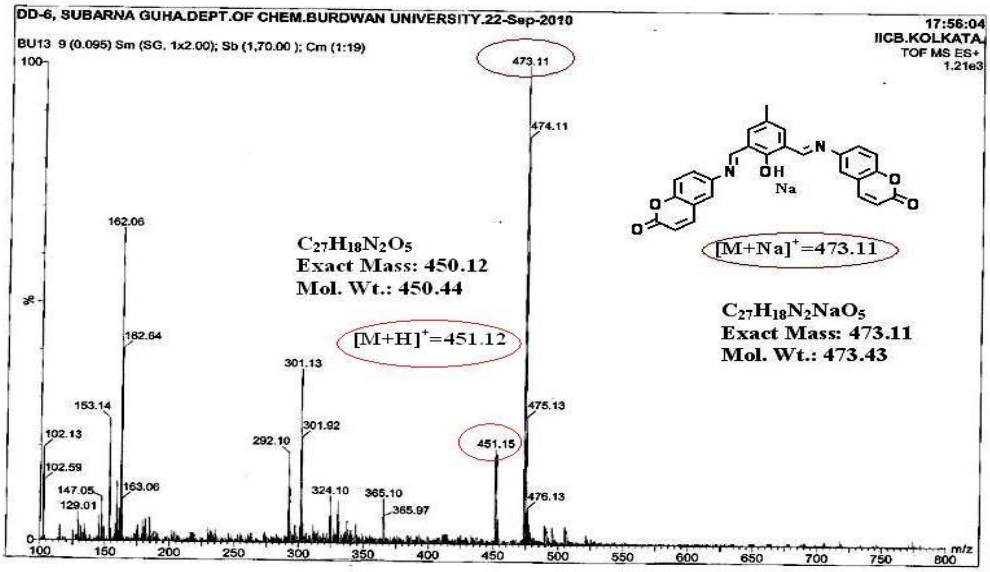

S-2. TOF MS ES (+) mass spectra of MCP

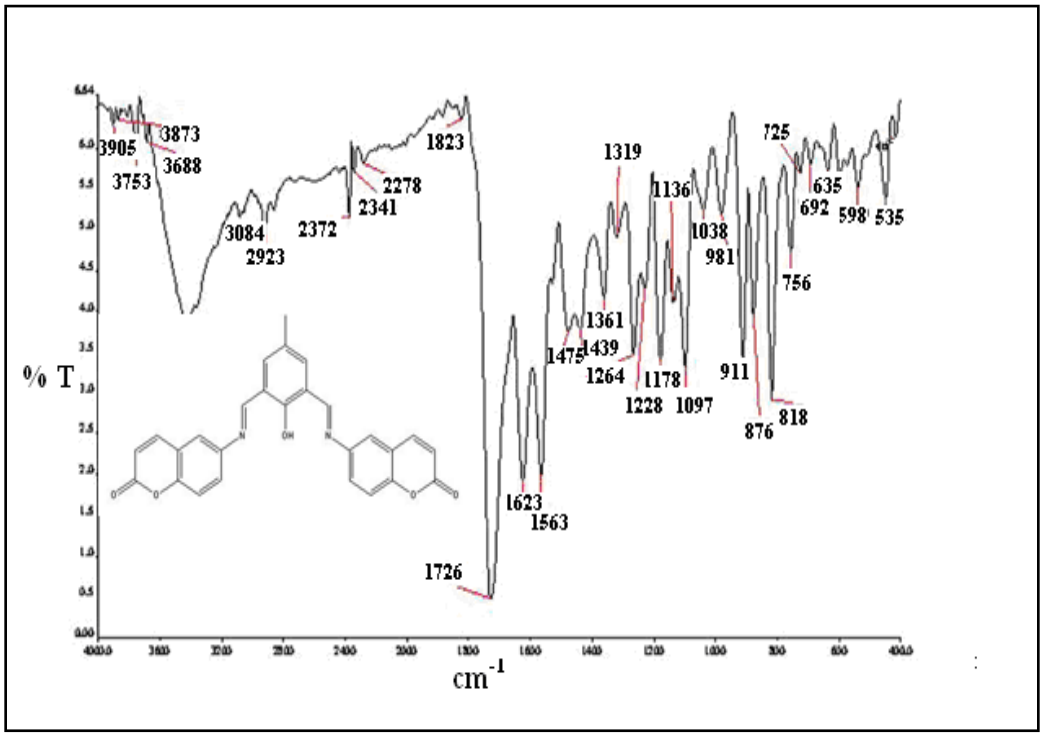

S-3. FTIR spectra of MCP

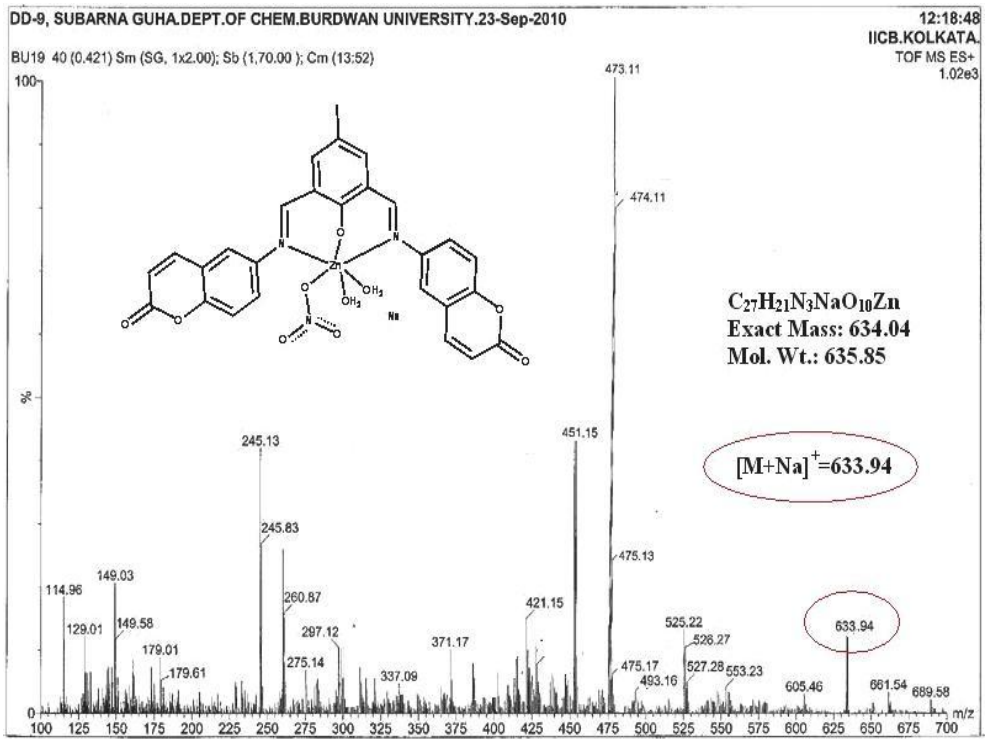

S-4. TOF MS ES (+) mass spectra of MCP-Zn^{2+}

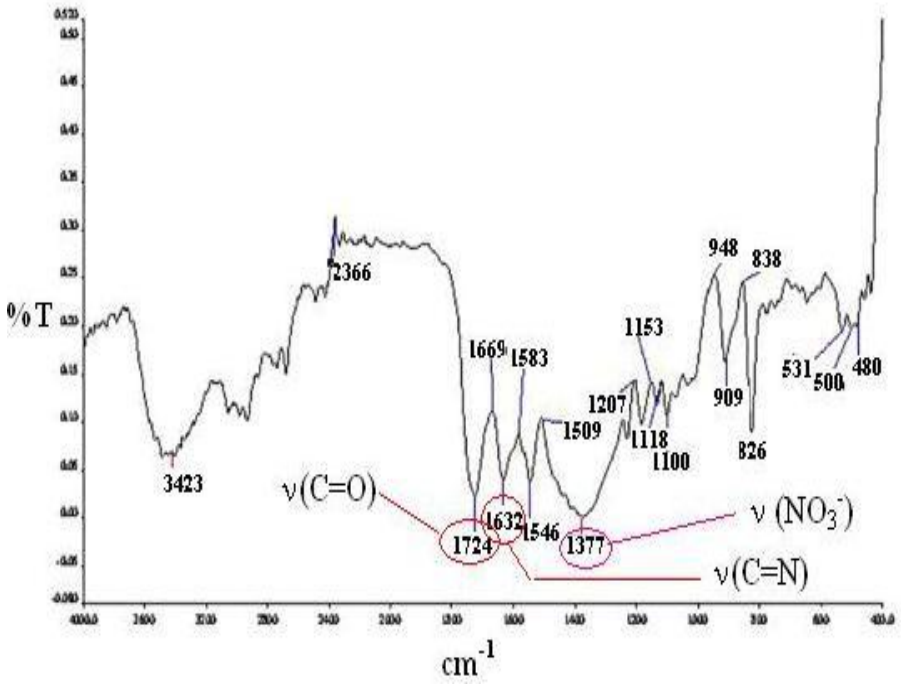

S-5. FTIR spectra of the MCP -Zn^{2+} complex

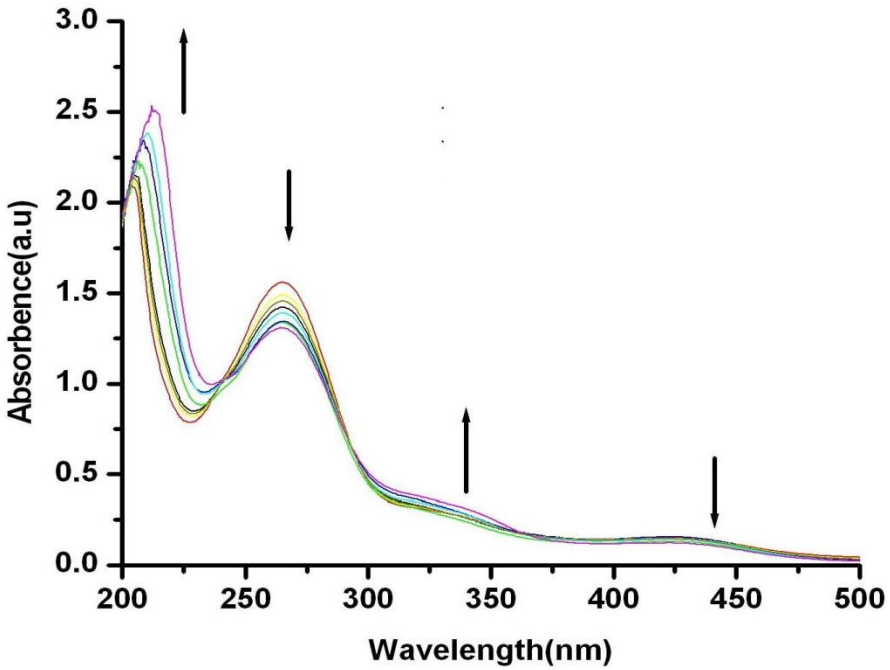

S-6. UV –Vis spectra of the ligand(MCP) and MCP -Zn^{2+} complex in methanol ([L] = 10^{-4} mol L^{-1}; [Complex] = [MCP - Zn^{2+}] = 10^{-4} mol L^{-1}.

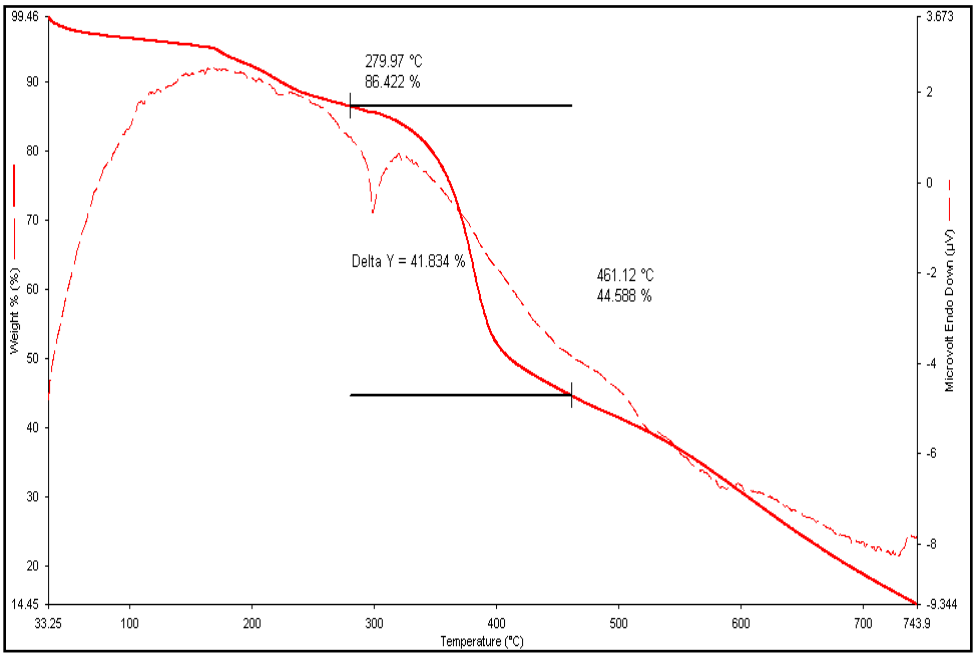

S-7.Thermogravimetry of MCP:

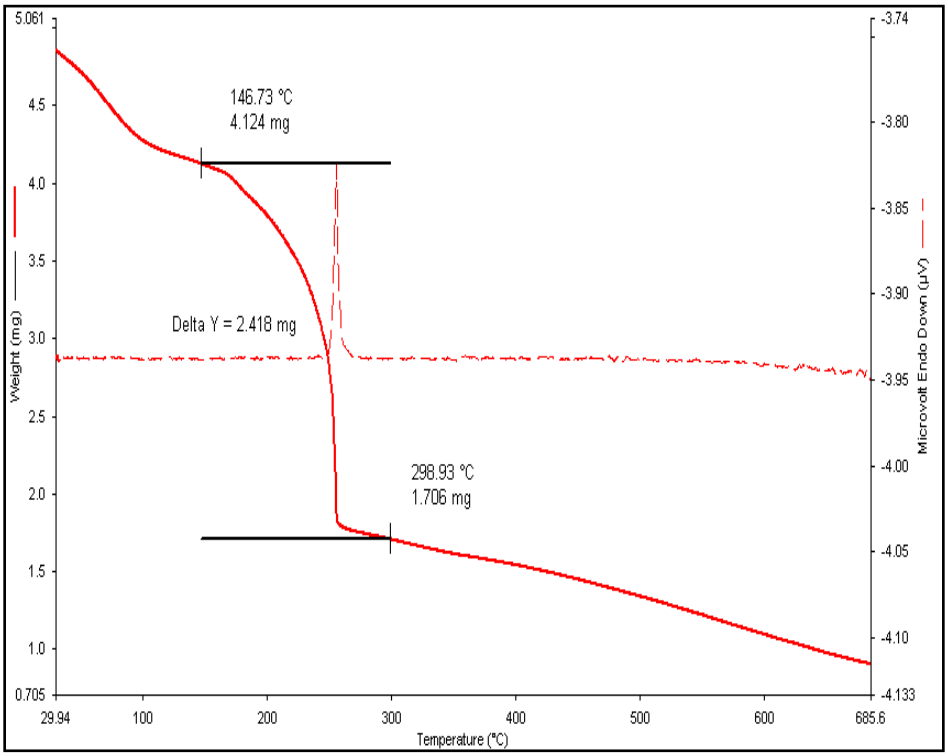

S-8.Thermogravimetry of MCP-Zn^{2+}

S9. Physical parameters of the MCP generated by Ab initio (Hartee Fock) method

Sum of Mulliken charges= 0.00000

Electronic spatial extent (au): <R**2>= 31695.0149

Charge= 0.0000 electrons

Dipole moment (field-independent basis, Debye):

X= -3.4372 Y= 7.4553 Z= 2.6692 Tot= 8.6326

Quadrupole moment (field-independent basis, Debye-Ang):

XX= -318.4945 YY= -181.2316 ZZ= -188.4173

XY= -15.3783 XZ= -8.5880 YZ= -3.9709

Traceless Quadrupole moment (field-independent basis, Debye-Ang):

XX= -89.1134 YY= 48.1495 ZZ= 40.9639

XY= -15.3783 XZ= -8.5880 YZ= -3.9709

Octapole moment (field-independent basis, Debye-Ang**2):

XXX= -303.3573 YYY= 72.6614 ZZZ= -4.1976 XYY= 96.0106

XXY= 520.5990 XXZ= 169.4148 XZZ= -17.2056 YZZ= -26.8025

YYZ= 17.7343 XYZ= -48.5106

Hexadecapole moment (field-independent basis, Debye-Ang**3):

XXXX=-54066.7502 YYYY= -5656.0861 ZZZZ= -785.3982 XXXY= -800.6052

XXXZ= -885.5790 YYYX= -288.8825 YYYZ= -20.0813 ZZZX= -22.9073

ZZZY= 17.3885 XXYY= -8177.4652 XXZZ= -5770.4224 YYZZ= -1110.0105

XXYZ= -346.6375 YYXZ= 98.8757 ZZXY= 8.8510

N-N= 2.932307328594D+03 E-N=-9.412178235342D+03 KE= 1.516482722213D+03

Table S10. Various bond lengths, angles and dihedral angles of MCP generated by Ab initio (Hartee Fock) method.

Row	Highlight	Tag	Symbol	NA	NB	NC	Bond	Angle	Dihedral	X	Y	Z
1	No	1	C							-0.4445340	2.0196800	0.1664720
2	No	2	C	1			1.4253476			-1.6696900	2.7170370	-0.0440080
3	No	3	C	2	1		1.3891586	119.6404020		-1.6475490	4.0811170	-0.3058420
4	No	4	C	3	2	1	2.3778349	91.6453379	5.1175603	0.7291240	4.0981840	-0.3781800
5	No	5	C	4	3	2	1.4090327	90.6292318	-0.6843102	0.7630550	2.7177650	-0.0977070
6	No	6	H	3	2	1	1.0759725	118.6154613	-177.5260080	-2.5836160	4.5987770	-0.4221330
7	No	7	H	4	3	2	1.0751987	150.7685939	175.7812145	1.6591560	4.6119460	-0.5429260
8	No	8	C	4	3	2	1.3850509	31.8369173	-178.3778794	-0.4557080	4.8109130	-0.4591520
9	No	9	C	8	4	3	1.5155922	122.2866809	-178.4285537	-0.4869780	6.3007510	-0.7356020
10	No	10	H	9	8	4	1.0849509	111.5012116	122.6332218	-1.0755140	6.5292020	-1.6179590
11	No	11	H	9	8	4	1.0852996	111.4332967	-117.1281985	-0.9165820	6.8495510	0.0963440
12	No	12	H	9	8	4	1.0830393	111.0768730	2.7247701	0.5112070	6.6873450	-0.9003620
13	No	13	C	2	1	5	4.7699835	107.2672585	146.7048914	-4.8828290	-0.4815050	-1.5265090
14	No	14	C	13	2	1	1.3856141	154.6324185	136.1812702	-6.1301290	-1.0844900	-1.5505540
15	No	15	C	14	13	2	1.3901825	118.8585681	-25.5466387	-6.9409910	-0.9939110	-0.4249850
16	No	16	C	15	14	13	1.3917771	121.5876317	-0.2236730	-6.5268920	-0.3186630	0.7193950
17	No	17	C	16	15	14	1.4016159	118.8952662	0.5448148	-5.2653260	0.2920180	0.7262470
18	No	18	C	17	16	15	1.3895416	120.4506102	0.2039980	-4.4452270	0.2266820	-0.3935720
19	No	19	H	13	2	1	1.0712923	83.0924061	-66.0430941	-4.2422130	-0.5357180	-2.3834450

20	No	20	H	14	13	2	1.0700576	121.8231940	154.6062322	-6.4825940	-1.6177650	-2.4086970
21	No	21	C	16	15	14	1.4584577	117.4507029	-178.8895220	-7.4396460	-0.3007540	1.8567860
22	No	22	H	17	16	15	1.0728139	119.4364508	-177.9666221	-4.9238220	0.7866680	1.6148560
23	No	23	C	21	16	15	1.3419487	121.0872127	-0.5337944	-8.6366320	-0.9041900	1.7942090
24	No	24	C	23	21	16	1.4714924	121.2744437	0.0560305	-9.0748030	-1.6077540	0.5783580
25	No	25	H	21	16	15	1.0723622	118.6490362	179.4702074	-7.1363510	0.2067250	2.7514580
26	No	26	H	23	21	16	1.0686558	123.0669114	-179.9731453	-9.3297280	-0.9103780	2.6076000
27	No	27	N	18	17	16	1.4243829	122.5392512	-178.7723100	-3.1456690	0.8088610	-0.4264870
28	No	28	O	24	23	21	1.3788386	115.6651806	0.3839266	-8.1770140	-1.6074040	-0.4681460
29	No	29	O	24	23	21	1.2100990	125.1467494	-179.6363782	-10.1384630	-2.1687370	0.4432100
30	No	30	C	5	4	3	8.5290926	115.3797864	-178.7771802	8.5545830	-0.6926720	0.5398130
31	No	31	C	30	5	4	2.4363762	25.1233864	-127.2423341	6.2790400	-0.5347880	-0.3162860
32	No	32	C	31	30	5	1.3922258	92.4237776	-19.8354058	5.8639930	0.2412760	0.7624880
33	No	33	C	32	31	30	1.4576073	117.5703404	-0.6969020	6.8504810	0.5509890	1.7898820
34	No	34	C	33	32	31	1.3419486	121.0578029	0.6336234	8.1150910	0.1133050	1.6897810
35	No	35	H	31	30	5	2.1305134	120.0058735	161.0988880	5.7540260	-1.5148490	-2.1336820
36	No	36	C	31	30	5	1.3896691	145.9189006	160.9719333	5.4028840	-0.9015900	-1.3306760
37	No	37	C	32	31	30	1.4011929	118.7105913	179.8640970	4.5307260	0.6696170	0.8100760
38	No	38	H	33	32	31	1.0724701	118.6831206	-179.2737288	6.5469440	1.1377090	2.6347590
39	No	39	H	34	33	32	1.0686508	123.1025204	-179.9173584	8.8639590	0.3197540	2.4236680
40	No	40	C	37	32	31	1.3878310	120.4307640	-0.2766929	3.6463980	0.3291170	-0.2038760
41	No	41	C	36	31	30	1.3863006	119.0337370	179.6963770	4.0863730	-0.4714190	-1.2708330
42	No	42	H	37	32	31	1.0731690	119.4952079	178.3458693	4.1905110	1.2458720	1.6490490
43	No	43	H	41	36	31	1.0691958	119.9563125	-179.0955843	3.3961070	-0.7569570	-2.0358040
44	No	44	N	40	37	32	1.4394167	120.6901814	-179.9287975	2.2759850	0.7673920	-0.1614070
45	No	45	O	30	5	4	1.3782311	52.2212006	-115.4351877	7.5860540	-0.9696620	-0.4007980
46	No	46	O	30	5	4	1.2102863	167.3740795	-64.6008185	9.6779400	-1.1110180	0.3729340
47	No	47	C	44	40	37	1.2946510	117.9474219	60.1078760	2.0467290	2.0414400	-0.1423100
48	No	48	C	27	18	17	1.2791235	120.6774175	-49.7064612	-2.9631140	2.0190850	-0.0547500
49	No	49	H	47	44	40	1.0812954	117.5537254	3.5179243	2.8978710	2.7040090	-0.2182000
50	No	50	H	48	27	18	1.0843166	119.5497991	-4.6580578	-3.8170680	2.6298440	0.2163190
51	No	51	Zn	44	40	37	2.1706586	119.5333552	-115.8058246	0.6871420	-0.7024380	0.0027160
52	No	52	O	1	5	4	1.3014569	121.3271190	-170.7027398	-0.4357820	0.7933000	0.6020240
53	No	53	O	51	44	40	2.0667172	99.8879705	-31.9982294	1.5474070	-2.2718820	-1.0307780
54	No	54	O	53	51	44	2.1858258	162.5369694	76.3318337	2.7979500	-3.9857040	-1.5568870
55	No	55	O	54	53	51	2.1944983	60.6602212	32.0448414	2.1745760	-3.7094740	0.5290000
56	No	56	N	54	53	51	1.2257827	31.3868274	31.9426370	2.1974810	-3.3537980	-0.6951010
57	No	57	O	51	44	40	2.0815364	132.0847776	-126.7896219	-1.0238590	-1.0400880	-1.1336210
58	No	58	H	57	51	44	0.9746765	112.8896629	-80.2609353	-1.7538530	-0.4346450	-0.9088060
59	No	59	H	57	51	44	0.9490787	129.9592026	105.8766942	-1.2133560	-1.7267240	-1.7608150
60	No	60	O	51	44	40	2.0486978	111.1485472	61.7616305	0.8436450	-1.7686310	1.7451000
61	No	61	H	60	51	44	0.9688019	112.9389950	-96.2072074	1.3041880	-2.6132760	1.6308540
62	No	62	H	60	51	44	0.9484391	129.6374157	89.8064441	0.4716900	-1.5901710	2.5991130

S11. Physical parameters of the MCP+Zn^{2+} generated by Ab initio (Hartee Fock) method

Sum of Mulliken charges= 0.00000

Electronic spatial extent (au): <R**2>= 35349.9527

Charge= 0.0000 electrons

Dipole moment (field-independent basis, Debye):

X= -4.4095 Y= 13.3776 Z= 5.1653 Tot= 15.0028

Quadrupole moment (field-independent basis, Debye-Ang):

XX= -392.2911 YY= -257.5383 ZZ= -221.5238

XY= 11.0087 XZ= 6.1095 YZ= -4.5943

Traceless Quadrupole moment (field-independent basis, Debye-Ang):

XX= -101.8400 YY= 32.9128 ZZ= 68.9272

XY= 11.0087 XZ= 6.1095 YZ= -4.5943

Octapole moment (field-independent basis, Debye-Ang**2):

XXX= 89.2893 YYY= 137.0604 ZZZ= 42.8977 XYY= -16.5326

XXY= 609.1416 XXZ= 257.3762 XZZ= -11.7085 YZZ= -51.0947

YYZ= 7.4217 XYZ= -10.9344

Hexadecapole moment (field-independent basis, Debye-Ang**3):

XXXX=-62008.0404 YYYY= -7488.1128 ZZZZ= -1439.0682 XXXY= -1434.3731

XXXZ= -184.4094 YYYX= 60.8414 YYYZ= -148.3124 ZZZX= 24.1364

ZZZY= 20.4472 XXYY= -9077.7457 XXZZ= -5997.9446 YYZZ= -1557.3327

XXYZ= 129.4115 YYXZ= 97.9558 ZZXY= 86.7407

N-N= 4.539703089692D+03 E-N=-1.387715340649D+04 KE= 2.061867305784D+03

Table S12. Various bond lengths, angles and dihedral angles of MCP+Zn^{2+} generated by Ab initio (Hartee Fock) method.

Row	Highlight	Tag	Symbol	NA	NB	NC	Bond	Angle	Dihedral	X	Y	Z
1	No	1	C							-0.4445340	2.0196800	0.1664720
2	No	2	C	1			1.4253476			-1.6696900	2.7170370	-0.0440080
3	No	3	C	2	1		1.3891586	119.6404020		-1.6475490	4.0811170	-0.3058420
4	No	4	C	3	2	1	2.3778349	91.6453379	5.1175603	0.7291240	4.0981840	-0.3781800
5	No	5	C	4	3	2	1.4090327	90.6292318	-0.6843102	0.7630550	2.7177650	-0.0977070
6	No	6	H	3	2	1	1.0759725	118.6154613	-177.5260080	-2.5836160	4.5987770	-0.4221330
7	No	7	H	4	3	2	1.0751987	150.7685939	175.7812145	1.6591560	4.6119460	-0.5429260
8	No	8	C	4	3	2	1.3850509	31.8369173	-178.3778794	-0.4557080	4.8109130	-0.4591520
9	No	9	C	8	4	3	1.5155922	122.2866809	-178.4285537	-0.4869780	6.3007510	-0.7356020
10	No	10	H	9	8	4	1.0849509	111.5012116	122.6332218	-1.0755140	6.5292020	-1.6179590
11	No	11	H	9	8	4	1.0852996	111.4332967	-117.1281985	-0.9165820	6.8495510	0.0963440
12	No	12	H	9	8	4	1.0830393	111.0768730	2.7247701	0.5112070	6.6873450	-0.9003620
13	No	13	C	2	1	5	4.7699835	107.2672585	146.7048914	-4.8828290	-0.4815050	-1.5265090
14	No	14	C	13	2	1	1.3856141	154.6324185	136.1812702	-6.1301290	-1.0844900	-1.5505540
15	No	15	C	14	13	2	1.3901825	118.8585681	-25.5466387	-6.9409910	-0.9939110	-0.4249850
16	No	16	C	15	14	13	1.3917771	121.5876317	-0.2236730	-6.5268920	-0.3186630	0.7193950
17	No	17	C	16	15	14	1.4016159	118.8952662	0.5448148	-5.2653260	0.2920180	0.7262470
18	No	18	C	17	16	15	1.3895416	120.4506102	0.2039980	-4.4452270	0.2266820	-0.3935720
19	No	19	H	13	2	1	1.0712923	83.0924061	-	-4.2422130	-0.5357180	-2.3834450

									66.0430941			
20	No	20	H	14	13	2	1.0700576	121.8231940	154.6062322	-6.4825940	-1.6177650	-2.4086970
21	No	21	C	16	15	14	1.4584577	117.4507029	-178.8895220	-7.4396460	-0.3007540	1.8567860
22	No	22	H	17	16	15	1.0728139	119.4364508	-177.9666221	-4.9238220	0.7866680	1.6148560
23	No	23	C	21	16	15	1.3419487	121.0872127	-0.5337944	-8.6366320	-0.9041900	1.7942090
24	No	24	C	23	21	16	1.4714924	121.2744437	0.0560305	-9.0748030	-1.6077540	0.5783580
25	No	25	H	21	16	15	1.0723622	118.6490362	179.4702074	-7.1363510	0.2067250	2.7514580
26	No	26	H	23	21	16	1.0686558	123.0669114	-179.9731453	-9.3297280	-0.9103780	2.6076000
27	No	27	N	18	17	16	1.4243829	122.5392512	-178.7723100	-3.1456690	0.8088610	-0.4264870
28	No	28	O	24	23	21	1.3788386	115.6651806	0.3839266	-8.1770140	-1.6074040	-0.4681460
29	No	29	O	24	23	21	1.2100990	125.1467494	-179.6363782	-10.1384630	-2.1687370	0.4432100
30	No	30	C	5	4	3	8.5290926	115.3797864	-178.7771802	8.5545830	-0.6926720	0.5398130
31	No	31	C	30	5	4	2.4363762	25.1233864	-127.2423341	6.2790400	-0.5347880	-0.3162860
32	No	32	C	31	30	5	1.3922258	92.4237776	-19.8354058	5.8639930	0.2412760	0.7624880
33	No	33	C	32	31	30	1.4576073	117.5703404	-0.6969020	6.8504810	0.5509890	1.7898820
34	No	34	C	33	32	31	1.3419486	121.0578029	0.6336234	8.1150910	0.1133050	1.6897810
35	No	35	H	31	30	5	2.1305134	120.0058735	161.0988880	5.7540260	-1.5148490	-2.1336820
36	No	36	C	31	30	5	1.3896691	145.9189006	160.9719333	5.4028840	-0.9015900	-1.3306760
37	No	37	C	32	31	30	1.4011929	118.7105913	179.8640970	4.5307260	0.6696170	0.8100760
38	No	38	H	33	32	31	1.0724701	118.6831206	-179.2737288	6.5469440	1.1377090	2.6347590
39	No	39	H	34	33	32	1.0686508	123.1025204	-179.9173584	8.8639590	0.3197540	2.4236680
40	No	40	C	37	32	31	1.3878310	120.4307640	-0.2766929	3.6463980	0.3291170	-0.2038760
41	No	41	C	36	31	30	1.3863006	119.0337370	179.6963770	4.0863730	-0.4714190	-1.2708330
42	No	42	H	37	32	31	1.0731690	119.4952079	178.3458693	4.1905110	1.2458720	1.6490490
43	No	43	H	41	36	31	1.0691958	119.9563125	-179.0955843	3.3961070	-0.7569570	-2.0358040
44	No	44	N	40	37	32	1.4394167	120.6901814	-179.9287975	2.2759850	0.7673920	-0.1614070
45	No	45	O	30	5	4	1.3782311	52.2212006	-115.4351877	7.5860540	-0.9696620	-0.4007980
46	No	46	O	30	5	4	1.2102863	167.3740795	-64.6008185	9.6779400	-1.1110180	0.3729340
47	No	47	C	44	40	37	1.2946510	117.9474219	60.1078760	2.0467290	2.0414400	-0.1423100
48	No	48	C	27	18	17	1.2791235	120.6774175	-49.7064612	-2.9631140	2.0190850	-0.0547500
49	No	49	H	47	44	40	1.0812954	117.5537254	3.5179243	2.8978710	2.7040090	-0.2182000
50	No	50	H	48	27	18	1.0843166	119.5497991	-4.6580578	-3.8170680	2.6298440	0.2163190
51	No	51	Zn	44	40	37	2.1706586	119.5333552	-115.8058246	0.6871420	-0.7024380	0.0027160

52	No	52	O	1	5	4	1.3014569	121.3271190	-170.7027398	-0.4357820	0.7933000	0.6020240
53	No	53	O	51	44	40	2.0667172	99.8879705	-31.9982294	1.5474070	-2.2718820	-1.0307780
54	No	54	O	53	51	44	2.1858258	162.5369694	76.3318337	2.7979500	-3.9857040	-1.5568870
55	No	55	O	54	53	51	2.1944983	60.6602212	32.0448414	2.1745760	-3.7094740	0.5290000
56	No	56	N	54	53	51	1.2257827	31.3868274	31.9426370	2.1974810	-3.3537980	-0.6951010
57	No	57	O	51	44	40	2.0815364	132.0847776	-126.7896219	-1.0238590	-1.0400880	-1.1336210
58	No	58	H	57	51	44	0.9746765	112.8896629	-80.2609353	-1.7538530	-0.4346450	-0.9088060
59	No	59	H	57	51	44	0.9490787	129.9592026	105.8766942	-1.2133560	-1.7267240	-1.7608150
60	No	60	O	51	44	40	2.0486978	111.1485472	61.7616305	0.8436450	-1.7686310	1.7451000
61	No	61	H	60	51	44	0.9688019	112.9389950	-96.2072074	1.3041880	-2.6132760	1.6308540
62	No	62	H	60	51	44	0.9484391	129.6374157	89.8064441	0.4716900	-1.5901710	2.5991130

Quantum yield measurement

The fluorescence quantum yield of the complex was determined using anthracene as a reference with a known ϕ_R value of 0.2 in methanol [1]. The complex and the reference dye were excited at same wavelength (430 nm), maintaining nearly equal absorbance (0.1) and the emission spectra. The area of the emission spectrum was integrated using the software available in the instrument and the quantum yield is calculated according to the following equation:

$$\phi_S/\phi_R = [A_S / A_R] \times [(Abs)_R /(Abs)_S] \times [\eta_S^2/\eta_R^2] \quad (1)$$

Here, ϕ_S and ϕ_R were the fluorescence quantum yield of the sample and reference respectively. A_S and A_R were the area under the fluorescence spectra of the sample and the reference respectively, $(Abs)_S$ and $(Abs)_R$ were the respective optical densities of the sample and the reference solution at the wavelength of excitation, and η_S and η_R are the values of refractive index for the respective solvent used for the sample and reference.

Reference

[1] D. F. Eaton, Pure Appl. Chem., 60 (1988) 1107.